

HeadLighter: Disentangling Illumination in Generative 3D Gaussian Heads via Lightstage Captures

Yating Wang^{1†} Yuan Sun^{2†} Xuan Wang² Ran Yi^{1*} Boyao Zhou² Yipengjing Sun²

Hongyu Liu² Yinuo Wang² Lizhuang Ma^{1*}

¹Shanghai Jiao Tong University ²AntGroup Research

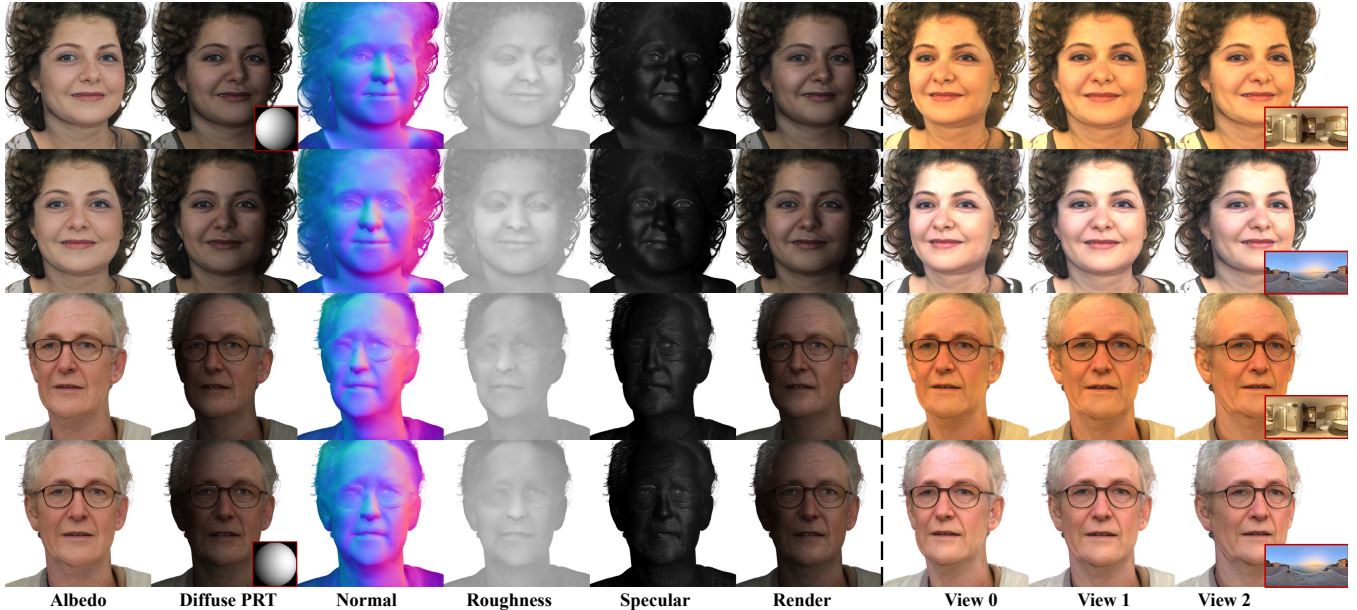


Figure 1: Our method achieves high-fidelity disentanglement of intrinsic appearance and illumination in generative 3D Gaussian head models. It produces photorealistic intrinsic attributes including albedo/normal/roughness and utilizes precomputed radiance transfer (PRT) for diffuse global shading, and supports relighting under diverse lighting conditions such as environment maps, spherical harmonics. Left: intrinsic appearance attributes of two generated subjects (rendered under the SH lighting shown in the red boxes). Right: relighting results under varying environment maps (shown in the red boxes).

Abstract

Recent 3D-aware head generative models based on 3D Gaussian Splatting achieve real-time, photorealistic and view-consistent head synthesis. However, a fundamental limitation persists: the deep entanglement of illumination and intrinsic appearance prevents controllable relighting. Existing disentanglement methods rely on strong assumptions to enable weakly supervised learning, which restricts their capacity for complex illumination. To address this challenge, we introduce HeadLighter, a novel supervised framework that learns a physically plausible decomposition of appearance and illumination in head generative models. Specifically, we design a dual-branch architecture that separately models lighting-invariant head attributes and physically grounded rendering components. A progressive disentanglement training is employed to gradually inject head appearance priors into the generative architecture, supervised by multi-view images captured under controlled light conditions with a light stage setup. We further introduce a distillation

strategy to generate high-quality normals for realistic rendering. Experiments demonstrate that our method preserves high-quality generation and real-time rendering, while simultaneously supporting explicit lighting and viewpoint editing. We will publicly release our code and dataset.

Keywords

Generative Heads, Face Relighting

ACM Reference Format:

Yating Wang^{1†} Yuan Sun^{2†} Xuan Wang² Ran Yi^{1*} Boyao Zhou² Yipengjing Sun² and Hongyu Liu² Yinuo Wang² Lizhuang Ma^{1*}, ¹Shanghai Jiao Tong University ²AntGroup Research, . 2026. HeadLighter: Disentangling Illumination in Generative 3D Gaussian Heads via Lightstage Captures. In . ACM, New York, NY, USA, 13 pages. <https://doi.org/10.1145/nnnnnnnnnnnnnnnn>

1 Introduction

Generative models for 3D human heads have seen remarkable progress, driven by their wide applications in digital avatars and virtual reality. Among them, the most prominent approaches are 3D-aware Generative Adversarial Networks (GANs) built upon

neural rendering techniques [Kerbl et al. 2023; Mildenhall et al. 2021]. These models learn a rich prior of 3D head geometry and appearance directly from large-scale 2D in-the-wild images, without requiring any explicit 3D supervision. Consequently, they can synthesize highly realistic and view-consistent 3D head with rich identity and appearance diversity. In the pursuit of real-time performance and impressive visual quality, recent works integrate 3D Gaussian Splatting (3DGS) into the generative framework [Barthel et al. 2025; Kirschstein et al. 2024], replacing the computationally intensive volume rendering and achieving real-time rendering.

However, a critical limitation persists: the illumination and the intrinsic head appearance (i.e., material or albedo) are deeply entangled, fundamentally preventing fine-grained control over the lighting conditions of the generated 3D heads. Existing approaches enable unsupervised decomposition of pretrained generative models using simplified reflectance models or strong assumptions. NFL [Jiang et al. 2023] involves style-mixing supervision with the white-light and face symmetry assumption, initializing from an on-the-shell light estimator, while GSHR [Lv et al. 2025] introduces a simplified light transport function for 3D gaussian and distills albedo and shading from NFL [Jiang et al. 2023]. Others [Deng et al. 2024; Ranjan et al. 2023] enforce physically plausible shading in neural volume rendering to split the diffuse and specular components. While these methods support explicit relighting, lack of real-world data supervision limits their ability to handle complex lighting and achieve highly physical plausibility.

We address this by an intuitive and straightforward way: involving a multi-view face dataset captured under controlled illuminations with a LightStage to learn the disentanglement. However, directly utilizing such dataset is non-trivial: compared to large-scale in-the-wild face image datasets, our light stage dataset covers only a limited range of identities and lighting conditions, and exhibits a noticeable domain gap relative to natural imagery. To prevent overfitting on the lightstage dataset and preserve the generalization capability of the base generative model, we decompose pretrained generative model into a dual-branch architecture: 1) a light-invariant base branch to generate geometry and albedo of 3D gaussian, and 2) a relight branch predicting attributes for physically-based rendering. To ensure stable disentanglement, we devise a progressive training strategy. First, we obtain base branch by fine-tuning the intermediate layers of a pretrained generator to remove illumination while preserving generation diversity. Next, with the base branch frozen, we inject head material priors from LightStage captures into the relight branch. Finally, we enhance the model’s generalization across diverse illumination environments by employing adversarial training with randomly sampled lighting conditions.

A further challenge lies in obtaining accurate surface normals, which are crucial for realistic shading but not native to 3D gaussian representations. While computing normals from extracted mesh or neighbor splats are feasible, such methods are computationally expensive in training iterations and can introduce significant noise. Observing that the base branch encodes face geometry, we task the relight branch to directly predict normals guided by base branch features. We further introduce a distillation strategy and smoothness terms that enforce consistent and plausible normal prediction, enabling photorealistic rendering of complex shading effects.

We demonstrate the effectiveness of our pipeline through comprehensive comparisons with state-of-the-art methods. We evaluate generative diversity, rendering speed and multi-view spatial consistency of our disentangled generative models. We demonstrate the rendering results of 3D human heads generated by our method under different lighting inputs. To further validate the disentanglement capability, we quantitatively and qualitatively compare free-view relighting results by extracting image pairs from our real-captured datasets. To foster future research, we will make our code and licensed dataset publicly available.

2 Related Works

2.1 3D-aware Generative Head Models

The pursuit of high-fidelity, view-consistent, and controllable 3D human head synthesis has led to the rapid evolution of 3D-aware Generative Adversarial Networks (GANs). These models learn to generate 3D heads from large-scale 2D image sets, bypassing the need for explicit 3D supervision. Early 3D GANs integrate various 3D representations [Chan et al. 2022, 2021; Schwarz et al. 2020; Sun et al. 2023; Tang et al. 2023] into the GAN framework. Among them, EG3D [Chan et al. 2022] utilizes a hybrid tri-plane representation, achieving photorealistic visual quality. However, its reliance on volume rendering is computationally expensive, and the super-resolution module can introduce view inconsistencies. To facilitate efficient, high-resolution generative head models, recent methods like [Barthel et al. 2025; Kirschstein et al. 2024; Yu et al. 2025] have turned to 3D Gaussian Splatting (3DGS) [Kerbl et al. 2023]. However, a fundamental limitation persists: intrinsic face appearance properties and lighting are conflated into a view-dependent color, which renders direct and physically plausible relighting impossible.

To enable explicit lighting control, a line of research [Deng et al. 2024; Jiang et al. 2023, 2025; Lv et al. 2025; Pan et al. 2021; Ranjan et al. 2023; Tan et al. 2022] has focused on disentangling illumination. NFL [Jiang et al. 2023] distills pseudo albedo and shading from a pretrained EG3D [Chan et al. 2022] model via style-mixing, constrained by white-light and face symmetry assumptions, along with an on-the-shelf light estimator. LumiGAN [Deng et al. 2024] and FaceLit [Ranjan et al. 2023] employ an inverse rendering framework to separately model diffuse and specular components. GSHR [Lv et al. 2025] achieves highly efficient synthesis by designing a simplified radiance transfer representation for 3D Gaussians, but it relies on supervision from pseudo-data generated by NFL [Jiang et al. 2023]. Consequently, these approaches lack access to ground-truth data and must resort to strong, simplifying assumptions that limit their ability to model the complex interaction between realistic materials and colored illumination. To address this, we propose HeadLighter, a high-fidelity relightable generative 3D Gaussian head model that learns illumination disentanglement from LightStage captures.

2.2 Portrait Relighting

Portrait relighting [Cai et al. 2024; Feng et al. 2021; Guo et al. 2025a; Hou et al. 2022; Mei et al. 2023; Pandey et al. 2021; Yeh et al. 2022] aims to render a person’s face under novel lighting conditions. The core challenge lies in solving an ill-posed inverse rendering

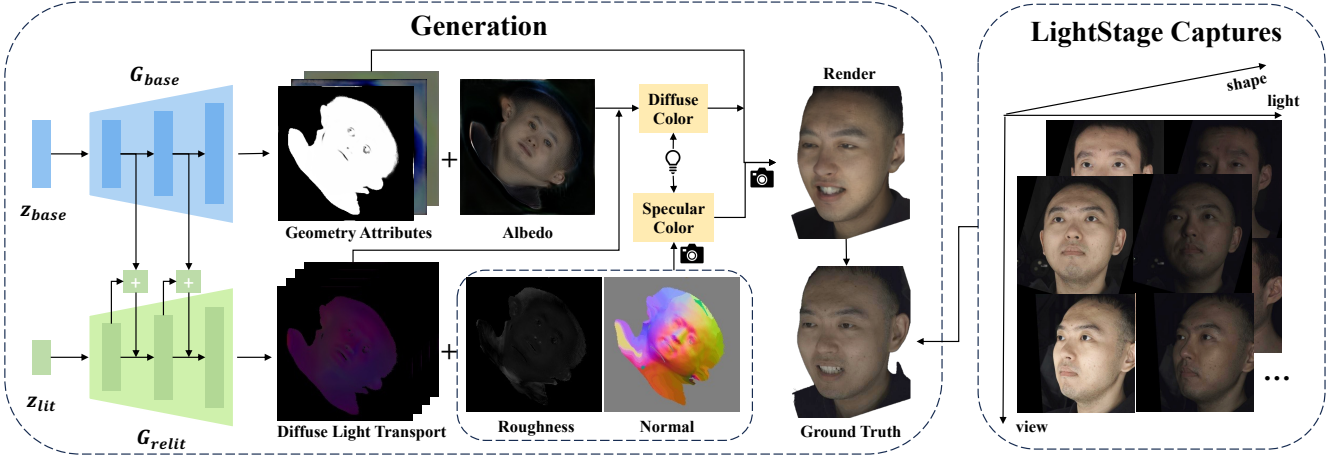


Figure 2: Our proposed framework. We leverage real-world captures to learn high-quality disentanglement of illumination and appearance in generative 3D gaussian heads. We capture multi-view images of different subjects under various light conditions via lightstage. A dual-branch architecture is employed to separately generate light-invariant gaussian attributes (geometry \mathcal{A}_{geo} and albedo ρ), and physically-based rendering attributes (normal n_k , roughness σ_k and diffuse light transport coefficients T_k). These attributes together with camera pose and light condition can be splatted into images and compared to the real-world captures to optimize the network.

problem to separate intrinsic properties from the scene’s illumination. Existing works [Debevec et al. 2000; Saito et al. 2024] capture One-Light-at-a-Time (OLAT) images with LightStage to enable rendering under novel lighting, yielding high-fidelity results. However, they require controlled capture settings and do not generalize to in-the-wild, sparse-view portraits. To enable relighting of in-the-wild portraits, subsequent methods introduce various priors and assumptions. Early works [Fei et al. 2024; Ponglertnapakorn et al. 2023; Zhou et al. 2019] rely on low-rank priors like 3D Morphable Models [Blanz and Vetter 2023]. Others [Chaturvedi et al. 2025; Wang et al. 2020; Yeh et al. 2022] leverage synthetic datasets for training but face a sim-to-real domain gap. SwitchLight [Kim et al. 2024] learns diffusion prior from OLAT data and synthetic data to enable single-image portrait relighting. Similarly, URAvatar [Li et al. 2024] learns shape and appearance priors from large-scale OLAT data to support relightable reconstruction from smartphone videos. Some works [Cai et al. 2024; Guo et al. 2025b; Mei et al. 2025] address portrait video relighting, focusing on consistency across frames. Moreover, some methods also attempt relighting for both human body [Teufel et al. 2025; Wang et al. 2025] and general scenes [Bharadwaj et al. 2025; Xing et al. 2025; Zhang et al. 2025].

Another line of research has shifted towards leveraging powerful generative priors. Initial attempts treated relighting as a style transfer task within the latent space of 2D GANs [Abdal et al. 2021; BR et al. 2021; Deng et al. 2020; Shoshan et al. 2021; Yi et al. 2024], but struggled to decouple illumination from other facial attributes like pose and expression. Recently, a growing body of work [Deng et al. 2024; Jiang et al. 2023; Lv et al. 2025; Mei et al. 2024; Pan et al. 2021; Rao et al. 2024, 2025; Tan et al. 2022] imposes generative 3D face priors to jointly support relighting and novel-view synthesis. HoloRelight [Mei et al. 2024] utilizes OLAT and synthetic data for training, first delighting the input and then applying new lighting conditions via an implicit shading representation. 3DPR [Rao et al.

2025] enables generating a basis of virtual OLAT images from a single portrait and then recombining them for relighting. Similar to NFL [Jiang et al. 2023] and GSHR [Lv et al. 2025], our method focuses on relightable 3D head generation but can also perform portrait relighting via an inversion-then-relight pipeline; however, under OLAT captures supervision, it achieves more physically accurate lighting disentanglement and thus better relighting quality.

3 Methods

3.1 Preliminaries

3D Head GAN leverages neural rendering techniques to learn priors of 3D facial shape and appearance from large-scale 2D image collections. To overcome the computational bottleneck of traditional volumetric rendering, recent works integrate the 3D GAN framework with fast rasterization of 3D Gaussian Splatting (3DGS) [Kerbl et al. 2023]. A prominent example is GGHead [Kirschstein et al. 2024], which employs a StyleGAN2-based generator [Karras et al. 2019] to map a latent code $z \in \mathbb{R}^{512}$ to multi-channel 2D attribute maps M_\star defined in the UV space of a template head mesh. The attributes for 3D Gaussian $\{G_k\}$, can be obtained by sampling the feature maps M_\star at UV coordinate x_k^{uv} . These attributes are categorized into: (1) geometry properties, including position $\mu_k \in \mathbb{R}^3$, rotation $q_k \in \mathbb{R}^4$, scale $s_k \in \mathbb{R}^3$, and opacity $o_k \in \mathbb{R}$; and (2) view-dependent radiance defined with 1-degree Spherical Harmonics (SH) $a_k \in \mathbb{R}^{3 \times (1+1)^2}$. The framework is further stabilized with several regularization terms during adversarial training.

3.2 Data Acquisition

We capture multi-view One-Light-A-Time(OLAT) images using LightStage system equipped with 46 calibrated uniform distributed

point lights and 28 synchronized cameras. Both the lights and cameras operate at 25 fps. We record under various lighting configurations, including a “Uniform” mode with all 46 lights turning on, a “Direction” mode where each light is activated together with its neighboring lights, and “Random” mode where 10 or 20 lights are randomly selected. To acquire accurate 2D detection for each frames, we insert a fully illuminated frame every 10 frames, assume the subject remains stationary across these 11 frames, and propagate its estimation to the intervening frames. We capture three expressions for each subject: neutral, eyes closed, and smile. More details about the dataset processing can be found in 4.1.

3.3 Relightable 3DGS Head Generation

We represent a relightable 3D head as a collection of 3D Gaussians $\{g_k\}$, where each Gaussian g_k is associated with a set of geometric and appearance attributes and can be rendered into an image via splatting in a differentiable, physically-based manner, given arbitrary lighting conditions and viewpoints. All attributes of the 3D Gaussians are embedded into structured 2D UV maps of a template head mesh, from which each Gaussian g_k samples its attributes at its assigned UV coordinate. We generate the geometry and material maps using a dual-branch StyleGAN generator. The two branches share a common UV parameterization but take distinct latent codes to disentangle geometry from lighting-specific attributes:

- **Base branch** $G_{\text{base}} : \mathbf{z}_{\text{base}} \rightarrow (\mathcal{A}_{\text{geo}}, \rho)$. It maps a latent code $\mathbf{z}_{\text{base}} \in \mathbb{R}^{512}$ to the geometric attributes $\mathcal{A}_{\text{geo}} = \{\mu_k, s_k, q_k, o_k\}$ and albedo ρ_k .
- **Relight branch** $G_{\text{relit}} : \mathbf{z}_{\text{lit}} \rightarrow (\mathbf{n}, \sigma, \mathbf{T})$. It takes a separate latent code $\mathbf{z}_{\text{lit}} \in \mathbb{R}^{128}$ to predict relighting-related attributes, including surface normals $\mathbf{n}_k \in \mathbb{R}^3$, scalar roughness σ_k , and diffuse light transport coefficients $\mathbf{T}_k \in \mathbb{R}^{3 \times (s+1)^2}$, where s denotes the SH degree.

Given incident lighting $\mathcal{L} = \{(\omega_i, \mathbf{I}_i)\}_{i=1}^M$, where ω_i denotes the direction of the i -th point light, and $\mathbf{I}_i \in \mathbb{R}^3$ denotes RGB radiance (encoding both color and intensity), the final color c_k of each Gaussian is computed as the sum of diffuse component $c_{\text{diffuse},k}(\mathcal{L})$ and specular component $c_{\text{specular},k}(\mathcal{L}, \omega_o)$, where ω_o is the viewing direction. Then the final color c_k and geometry attributes \mathcal{A}_{geo} of 3D Gaussians can be rendered into images via efficient splatting, enabling high-fidelity, and relightable head synthesis under arbitrary illumination.

Specifically, for the view-independent **diffuse** term $c_{\text{diffuse},k}$, we adopt Precomputed Radiance Transfer (PRT) [Sloan et al. 2002] to model global illumination effects, including self-occlusion and subsurface scattering. The illumination from each light source is projected into SH coefficient vectors $\mathbf{L}_i \in \mathbb{R}^{(s+1)^2}$. The network predicts per-Gaussian diffuse transport coefficients \mathbf{T}_k , and the diffuse color is calculated by inner products in SH domain, modulated by the albedo ρ_k :

$$c_{\text{diffuse},k}(\mathcal{L}) = \rho_k \odot \sum_{i=1}^M (\mathbf{T}_k \cdot \mathbf{L}_i). \quad (1)$$

The view-dependent **specular** term $c_{\text{specular},k}$ is modeled using a simplified Cook-Torrance microfacet model [Cook and Torrance 1981] to create realistic highlights. The total specular radiance is

the sum of contributions from all M light sources:

$$c_{\text{specular},k}(\mathcal{L}, \omega_o) = \sum_{i=1}^M f_{\text{specular}}(\omega_i, \omega_o, \mathbf{n}_k) (\mathbf{n}_k \cdot \omega_i) \mathbf{I}_i, \quad (2)$$

where the specular BRDF f_{specular} is defined as:

$$f_{\text{specular}}(\omega_i, \omega_o, \mathbf{n}_k) = \frac{D(\mathbf{h}_i, \alpha_k) F(\omega_o, \mathbf{h}_i) G(\omega_i, \omega_o, \alpha_k)}{4 (\mathbf{n}_k \cdot \omega_i) (\mathbf{n}_k \cdot \omega_o)}, \quad (3)$$

Here, $\mathbf{h}_i = \frac{\omega_i + \omega_o}{\|\omega_i + \omega_o\|}$ is the halfway vector for the i -th light source. The D term is modeled by the Trowbridge-Reitz GGX distribution [Trowbridge and Reitz 1975] parameterized by the per-Gaussian roughness σ_k :

$$D(\mathbf{h}_i) = \frac{\alpha_k^2}{\pi((\mathbf{n}_k \cdot \mathbf{h}_i)^2(\alpha_k^2 - 1) + 1)^2}, \quad \alpha_k = \sigma_k^2. \quad (4)$$

The Fresnel term F is computed using Schlick’s approximation [Schlick 1994]

$$F(\omega_o, \mathbf{h}_i) = F_0 + (1 - F_0)(1 - \max(\omega_o \cdot \mathbf{h}_i, 0))^5, \quad (5)$$

with a fixed dielectric Fresnel base reflectance $F_0 = 0.04$ for the entire head, consistent with skin and hair materials. The geometry term G follows the Smith masking-shadowing model for GGX as described in [Walter et al. 2007].

3.4 Disentanglement

Our goal is to disentangle intrinsic head appearance and extrinsic illumination in a generative 3D Gaussian head model, supervised by high-fidelity lightstage captures. To achieve stable training, we devise a three-stage training strategy: (1) The first stage trains the base branch G_{base} , adapting a pretrained entangled generator to light-invariant domain. (2) Based on the guidance of the base branch, the second stage trains the relight branch G_{relit} , learning the interaction between incident light and head surfaces using the captured lightstage data. (3) To generalize our model to arbitrary illumination beyond the limited white-light OLAT data, we apply adversarial loss on images rendered with randomly sampled lighting.

3.4.1 Stage 1: Base Branch Adaptation. We initialize G_{base} by adapting a pretrained head generative model, GGHead [Kirschstein et al. 2024] to produce \mathcal{A}_{geo} and view-independent albedo ρ_k , while maintaining its diversity of high-quality generation. GGHead does not decouple intrinsic appearance and scene illumination, and its color output – first-order SH coefficients per RGB channel – represents a view-dependent radiance that entangles both factors. We firstly modify GGHead to output 3-channel RGB colors instead of the original 12-channel SH coefficients. The modified generator is first finetuned on the FFHQ dataset (with segmentation masks derived from SAM [Kirillov et al. 2023] and [Zheng et al. 2024]) using an adversarial loss, which enforces a view-independent radiance, discarding anisotropic shading components at the base level. Subsequently, it is finetuned for 20k iterations using pseudo albedo images generated by [Jiang et al. 2023] via adversarial loss. Instead of updating all layers, we restrict updates to the intermediate layers (specifically, layer 5 and 6 in the GGHEAD backbone). These intermediate layers are known to encode mid-level appearance features such as shading and illumination [Karras et al. 2019]. This targeted

adaptation steers the generator toward the albedo domain while preserving high-level identity structure and face details, and the limited training duration further mitigates the risk of collapsing to the limited pseudo albedo images.

3.4.2 Stage 2: Relight Priors from LightStage Captures. Stage 2 focuses on training the relight branch G_{relit} , while keeping the base generator G_{base} frozen. We first implement multi-view GAN inversion on G_{base} to obtain geometry and albedo of lightstage captures. We then optimize G_{relit} and latent code per subject to predict relighting-related attributes $(\mathbf{n}_k, \sigma_k, \mathbf{T}_{d,k})$ that match the lightstage observations, where the multi-scale features output by G_{base} are injected into G_{relit} as a guidance. A novel normal distillation strategy is proposed to predict high-quality normal. We further utilize several regularization terms to constrain the generated attributes to be plausible.

Geometry and Albedo Inversion. Given an image sequence captured under varying lighting, we perform multi-view GAN inversion on the fully illuminated frame and propagate the results to the following frames. Specifically, we optimize implicit latent code $\mathbf{w}^+ \in \mathbb{R}^{512 \times L}$ in the extended \mathcal{W}^+ space of StyleGAN2 to yield per-Gaussian attributes \mathcal{A}_{geo} and albedo ρ_k , as well as intermediate feature maps $\{\mathbf{F}_{\text{base}}^l\}_{l=1}^L$ from G_{base} . We use L2 loss and perceptual loss to constrain the multi-view inversion, and image total variance loss to avoid holes during gaussian rendering:

$$\mathcal{L}_{\text{inv}} = \mathcal{L}_2 + \mathcal{L}_{\text{perc}} + \mathcal{L}_{\text{tv}}. \quad (6)$$

Notably, unlike methods such as PTI [Roich et al. 2022] that fine-tune the generator weights per subject, our approach keeps the base generator G_{base} fixed throughout inversion to preserve consistent feature representations across different identities in the latent space.

Multi-Scale Feature Guidance. Observing that early layers of G_{base} encode coarse shape (informing global illumination effects), while later layers capture fine details (crucial for normals and roughness), we leverage multi-scale features $\{\mathbf{F}_{\text{base}}^l\}_{l=1}^L$ of G_{base} to guide the relight branch. Specifically, a lightweight fusion network Φ^l predicts a residual update Δ^l from the concatenation of the current features of relight branch $\mathbf{F}_{\text{relit}}^l$ and the instance-normalized base branch feature $\mathbf{F}_{\text{base}}^l$:

$$\mathbf{F}_{\text{relit}}^l = \mathbf{F}_{\text{relit}}^l + \Delta^l, \quad \Delta^l = \Phi^l(\mathbf{F}_{\text{base}}^l, \mathbf{F}_{\text{relit}}^l). \quad (7)$$

This guidance enables G_{relit} to predict relighting attributes consistent with the underlying geometry and albedo from G_{base} while ensuring robust training.

Normal Prediction. Notably, 3DGS does not provide native normals, which are critical for view-dependent specular rendering. One viable method is to extract an explicit mesh from the 3D Gaussian splats and assign nearest face normal to each splat. But mesh extraction for each training iteration is computationally expensive, and the recovered surfaces are sensitive to noise of gaussian splats. An alternative is to use k-NN search to find neighboring splats and compute average orientation as the normal, which is even more susceptible to noise. Since our G_{base} module generates high-quality geometry, its output features $\{\mathbf{F}_{\text{base}}^l\}_{l=1}^L$ implicitly contain the geometry information, which could serve as cues for predicting normals. As we have injected the multi-scale base branch feature $\{\mathbf{F}_{\text{base}}^l\}_{l=1}^L$

into the relight branch, we propose to directly use G_{relit} to predict the normals, adding 3 channels to its output as the normal map.

To ensure the correctness and smoothness of the predicted normals, we introduce a self-distillation loss and 2D smoothness term. Based on the inverted geometry represented by gaussian point clouds, we pre-extract meshes via poisson reconstruction and cleanup the noise hair region by projecting onto 2D skin-parsing [Yakhyokhuja 2024] masks. Let $\hat{\mathbf{n}}_k^{\text{mesh}}$ be the closest mesh triangle normal of the gaussian splat g_k . We minimize the angular deviation between normalized normal prediction \mathbf{n}_k and $\hat{\mathbf{n}}_k^{\text{mesh}}$ via cosine similarity:

$$\mathcal{L}_{\text{normal}}^D = \frac{1}{N} \sum_{k=1}^N (1 - \mathbf{n}_k^\top \hat{\mathbf{n}}_k^{\text{mesh}}). \quad (8)$$

For the noisy hair region, we utilize a 2D Total Variation loss. We render the normalized normals \mathbf{n}_k as RGB colors of gaussian and splat them to a 2D normal map $I_{\text{norm}} \in \mathbb{R}^{H \times W \times 3}$, and apply total variation regularization:

$$\mathcal{L}_{\text{normal}}^{\text{TV}} = \|\nabla_x I_{\text{norm}}\|_1 + \|\nabla_y I_{\text{norm}}\|_1, \quad (9)$$

where ∇_x and ∇_y denote horizontal and vertical finite differences.

Training. The final loss of Stage 2 consists of shading loss, the aforementioned normal prediction loss and a regularization term on diffuse transport coefficients \mathbf{T}_k . We use these losses to optimize parameters of G_{relit} and a latent code $\mathbf{w}_{\text{lit}}^+ \in \mathbb{R}^{512 \times L}$ to represent per-subject head appearance properties.

The shading loss is formulated in Eq. (10), where $\mathcal{L}_{\text{tv}}^I$ is involved to prevent image noise.

$$\mathcal{L}_{\text{shading}} = \mathcal{L}_{\text{img}} + \mathcal{L}_{\text{perc}} + \mathcal{L}_{\text{tv}}^I. \quad (10)$$

To encourage spectrally smooth diffuse response, we regularize the diffuse transport coefficients $\mathbf{T}_k \in \mathbb{R}^{3 \times 9}$ by minimizing the variance across the RGB channels:

$$\mathcal{L}_{\text{prt}} = \frac{1}{N} \sum_{k=1}^N \|\mathbf{T}_k - \bar{\mathbf{T}}_k\|_2^2, \quad \bar{\mathbf{T}}_k = \frac{1}{3} \sum_{c \in \{r,g,b\}} \mathbf{T}_k^{(c)}. \quad (11)$$

3.4.3 Stage3: Adversarial Training. In this final stage, we perform adversarial training to ensure robust photorealism under arbitrary illumination. Given that our dataset consists solely of limited white-light OLAT captures, we employ adversarial supervision on images generated with randomly sampled illumination. This strategy expands the training distribution, ensuring the model generalizes well to diverse illumination environments.

First, to support random sampling of the relight latent code, we initialize mapping network M_{lit} that maps a randomly sampled code $\mathbf{z}_{\text{lit}} \in \mathbb{R}^{128}$ into the \mathcal{W}^+ space of G_{relit} , utilizing the optimized $\mathbf{w}_{\text{lit}}^+$ from Stage 2 as training data. Subsequently, we freeze the parameters of the base branch G_{base} , exclusively optimizing the synthesis network of G_{relit} . During each training iteration, we simulate diverse illumination conditions to broaden the lighting manifold beyond the training set. We pre-define a set of candidate point lights uniformly distributed on the hemisphere frontal to the face. A random lighting condition $\mathcal{L}_{\text{rand}}$ is constructed by randomly sampling a subset of candidate lights and assigning random RGB intensities to each source. Simultaneously, we sample random latent codes \mathbf{z}_{base} for the geometry representation and random \mathbf{z}_{lit} for the materials. The relight branch G_{relit} synthesizes the relighted

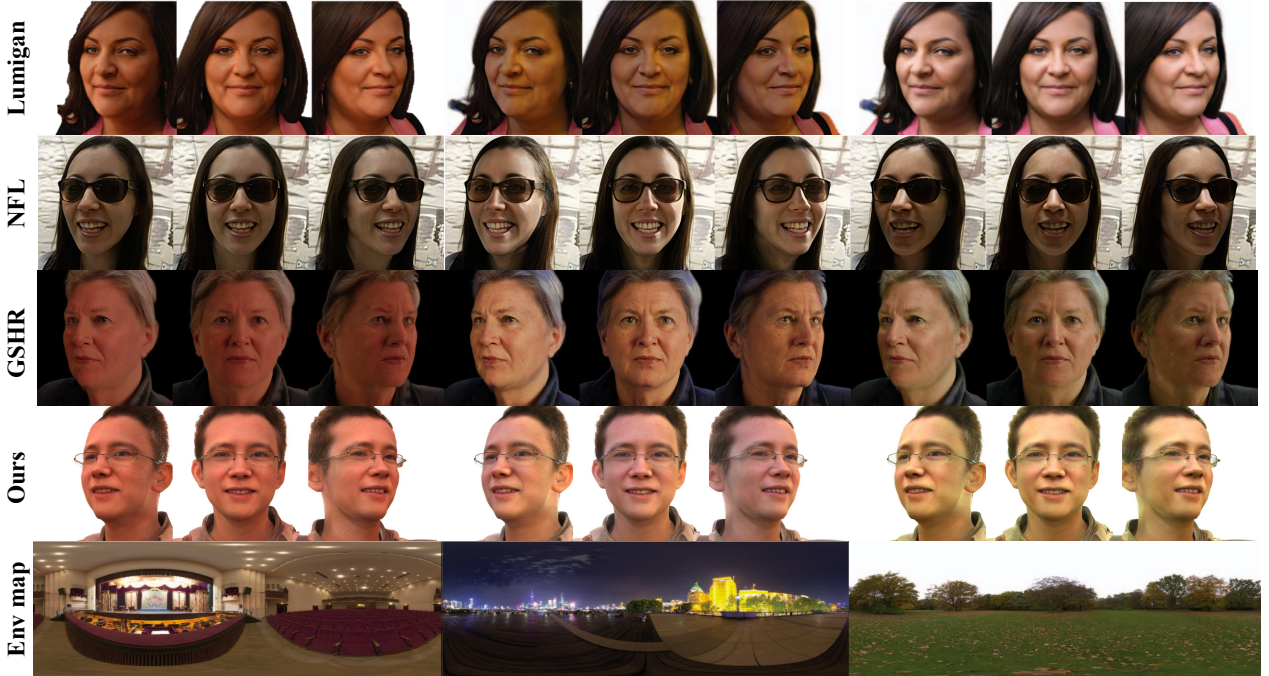


Figure 3: Relighting under complex environment maps. LuminGAN [Deng et al. 2024] and NFL assumes white illumination and fails to handle colored lighting. GSHR lacks real-world OLAT supervision and therefore cannot produce correct responses under non-uniform colored lighting. In contrast, our method accurately reproduces spatially varying lighting effects.

Method	SR	Relit	FID \downarrow	FPS \uparrow
EG3D	✓	✗	4.30	42
GGHead	✗	✗	4.87	228
NFL	✓	✓	4.16	2.8
GSHR	✗	✓	5.71	243
Ours	✗	✓	4.78	201

Table 1: Comparison of generative quality and rendering speed. SR denotes super resolution modules and Relit denotes whether to support explicit lighting control. Rendering speed is tested on Nvidia A6000 GPU.

head image using these random inputs, which is then supervised by an adversarial loss using pretrained discriminator of GGHead. This supervision guides the generator to produce high-fidelity, photorealistic textures that remain stable under varying, colored synthetic lighting. Moreover, the losses from Stage 2 are retained in this final stage to serve as a regularizer to prevent the relight branch from drifting. To ensure stable fine-tuning, we employ a reduced learning rate of 1×10^{-6} .

4 Experiments

4.1 Implementation Details.

Lightstage Dataset. We first perform calibration to obtain the world coordinates of each point light and camera. For the captured multi-view images, we use open-source tools to detect 2D

landmarks [Bulat and Tzimiropoulos 2017] and human segmentation [Zheng et al. 2024] for the "Uniform" frame. All the frames are aligned and cropped into 512 resolution. The head pose for each frame is solved using multi-view 2D landmarks and calibrated camera extrinsics, constrained by a 3DMM prior [Paysan et al. 2009]. 56 participants (31 male, 25 female) perform three expressions (neutral, smile, and eyes closed), each recorded under 95 distinct lighting configurations. We select 46 subjects for training and 10 for testing. **Architecture and Training.** G_{relit} shares the same overall architecture and number of layers as the G_{base} . However, since G_{base} models complex geometric and appearance details that go far beyond head reflectance alone, we design G_{relit} with reduced capacity: the convolutional layers in G_{relit} operate on features of up to 256 dimensions, compared to up to 512 dimensions in G_{base} . Correspondingly, we use a 128-dimensional latent code \mathbf{z}_{lit} to represent head material properties, while geometry and intrinsic appearance are encoded by a 512-dimensional latent code \mathbf{z}_{base} . During Stage 2, G_{relit} is optimized with Adam using a learning rate of 5×10^{-4} , while the lighting latent code \mathbf{w}_{lit} is updated with a higher learning rate of 1×10^{-3} . Additional details are provided in the supplementary material.

4.2 3D Generation.

We evaluate generation quality against multiple state-of-the-art 3D-aware head synthesis methods. First, we assess *generation diversity* by generating 50K images and computing FID against the FFHQ dataset [Kazemi and Sullivan 2014]. Images are rendered under random lighting conditions synthesized as described in Stage 3. Second, we measure *rendering speed* on a NVIDIA A6000 GPU.

Method	PSNR \uparrow	SSIM \uparrow	LPIPS \downarrow
EG3D	29.29	0.9026	0.065
GGHead	31.53	0.9085	0.052
NFL	30.02	0.9002	0.058
GSHR	30.64	0.8890	0.062
Ours	32.09	0.9132	0.050

Table 2: Evaluation of spatial consistency of generated 3D heads. We render multi-view images from the generated 3D heads and synthesis novel view using NeuS2 [Wang et al. 2023]; higher PSNR, SSIM, and lower LPIPS indicate better spatial consistency.

Third, we evaluate *multi-view spatial consistency*: for a random latent code, we render 30 viewpoints across -45° to 45° , hold out the frontal view as ground truth to calculate metrics, and use the remaining views to reconstruct the geometry by NeuS2 [Wang et al. 2023].

We compare with four baselines: EG3D [Chan et al. 2022] and NFL [Jiang et al. 2023], which rely on neural volume rendering, and GGHead [Kirschstein et al. 2024], GSHR [Lv et al. 2025], which are built upon 3D Gaussian splatting. Among them, EG3D and GGHead do not support explicit illumination control while NFL and GSHR support lighting control. We show the FID score and rendering FPS in Table 1. Methods based on 3D Gaussian achieve significantly higher rendering speeds than volume-rendering counterparts. Our method is slightly slower than GGHead due to the physically-based shading model but maintains the real-time rendering performance. We evaluate multi-view consistency using a wide viewport range ($\pm 45^\circ$). Our method achieves plausible disentanglement, which eliminates the inconsistent anisotropic artifacts, thus produces better multi-view consistency, as shown in Table 3.

4.3 Light Control.

We compare the rendering performance of various generative methods under complex and extreme illumination conditions. The baselines include LumiGAN [Deng et al. 2024], NFL [Jiang et al. 2023], and GSHR [Lv et al. 2025]. While LumiGAN and NFL are restricted by a white-light assumption, both GSHR and our method support colored illumination. Since LumiGAN’s code is unavailable, its results are sourced from the original paper. Figure 3 illustrates the results under non-uniform colored environment maps. Our generated 3D heads accurately respond to spatially-varying environmental lighting. Furthermore, Figure 4 demonstrates relighting results under extreme conditions, such as side-lighting or low-light environments. Lacking supervision from real-world data, NFL and GSHR fail to handle these extreme cases, either producing significant artifacts or failing to respond. In contrast, our method produces high-fidelity shadow and specular highlights.

4.4 Portrait Relighting.

Our method, along with NFL and GSHR, enable generating 3D human heads and support portrait illumination and viewport editing

Method	PSNR \uparrow	SSIM \uparrow	LPIPS \downarrow
NFL	24.6011	0.8227	0.1179
GSHR	20.0688	0.7464	0.1907
Lite2Relight	20.8874	0.8073	0.1278
Ours	27.0550	0.8614	0.1001

Table 3: Quantitative comparisons of free view relighting.

via 3D GAN inversion. To validate our model’s ability to disentangle illumination and appearance, we extract image pairs from LightStage captures and perform free-view relighting using our method and baselines. We also compare against Lite2Relight[Rao et al. 2024], a recent 3D GAN based portrait editing method. For 10 test subjects, we randomly sample two types of OLAT image pairs: one from uniform illumination to side lighting (as shown in the first row of Fig 5), and the other from side lighting to uniform illumination (shown in the second row of Fig 5), with 10 random lighting combinations for each type. Our method demonstrates superior robustness in handling low-light environments and extreme side-lighting. We also provide quantitative results in Tab 3.

4.5 Ablation Study.

Base Branch Adaption. We fine-tune GGHead with NFL-generated pseudo-albedo images to remove illumination, optimizing only intermediate layers to avoid identity collapse. We compare results before and after optimization using the same latent code, as shown in Fig 6. From left to right: the original GGHead output, optimization of layer 6, optimization of two intermediate layers 5 and 6, and full-model optimization. Full-model optimization significantly alters facial geometry, biasing it toward the average face. Optimizing only the 6th layer fails to fully remove illumination artifacts. Our method effectively removes illumination while preserving coarse face structure and fine-grained details.

Normal Distillation. We show the normal calculation results of different methods in Fig 9. Directly computing normals from neighboring points in gaussian splats introduces significant noise, making it unsuitable for photorealistic rendering. Reconstructing a mesh from the Gaussian point cloud and then extracting normals is computationally expensive to the training process and often produces noticeable artifacts in fine regions such as hair. To address this, we directly predict normals using the G_{relit} branch, supervised by normals derived from a pre-extracted mesh combined with a 2D total variation loss, yielding smooth and accurate surface normals.

Random Light and Adversarial Training. We evaluate the impact of random illumination and adversarial training by comparing rendering results under novel, colored lighting conditions not present in the white-light OLAT training set. As shown in Fig 8, without this stage, the model exhibits noticeable artifacts and color inconsistencies when subjected to non-uniform illumination. By incorporating adversarial training with randomly sampled lighting, our method ensures well generalization to diverse lighting, producing stable and realistic relighting results under challenging, unseen conditions.

Explicit Control on Roughness. Our method generates disentangled and physically-based face material properties. To evaluate the quality of disentanglement, we perform direct attribute editing on the roughness component. As illustrated in Figure 7, decreasing

the roughness value leads to more pronounced specular highlights while preserving other appearance attributes, demonstrating effective decoupling of the material properties.

5 Conclusion.

We propose a novel framework to disentangle illuminations and intrinsic appearances within a 3D gaussian head generative model supervised by high-fidelity lightstage captures. We utilize a dual-branch architecture to predict geometry with albedo and shading attributes, and employ a progressive training schema to ensure stable training. We further propose a normal supervision method to produce high-quality normals which are crucial for realistic rendering. Experiments demonstrate the generation ability and rendering speed of our method, validate the quality of disentanglement by light and viewport control.

References

Rameen Abdal, Peihao Zhu, Niloy J Mitra, and Peter Wonka. 2021. Styleflow: Attribute-conditioned exploration of stylegan-generated images using conditional continuous normalizing flows. *ACM Transactions on Graphics (ToG)* 40, 3 (2021), 1–21.

Florian Barthel, Wieland Morgenstern, Paul Hinzer, Anna Hilsmann, and Peter Eisert. 2025. CGS-GAN: 3D Consistent Gaussian Splatting GANs for High Resolution Human Head Synthesis. *arXiv preprint arXiv:2505.17590* (2025).

Shrishti Bharadwaj, Haiwen Feng, Giorgio Becherini, Victoria Fernandez Abrevaya, and Michael J Black. 2025. GenLit: Reformulating single-image relighting as video generation. In *Proceedings of the SIGGRAPH Asia 2025 Conference Papers*. 1–12.

Volker Blanz and Thomas Vetter. 2023. A morphable model for the synthesis of 3D faces. In *Seminal Graphics Papers: Pushing the Boundaries, Volume 2*. 157–164.

Mallikarjun BR, Ayush Tewari, Abdallah Dib, Tim Weyrich, Bernd Bickel, Hans-Peter Seidel, Hanspeter Pfister, Wojciech Matusik, Louis Chevallier, Mohamed Elgharib, et al. 2021. Photoapp: Photorealistic appearance editing of head portraits. *ACM Transactions on Graphics* 40, 4 (2021), 1–16.

Adrian Bulat and Georgios Tzimiropoulos. 2017. How far are we from solving the 2D & 3D Face Alignment problem? (and a dataset of 230,000 3D facial landmarks). In *International Conference on Computer Vision*.

Ziqi Cai, Kaiwen Jiang, Shu-Yu Chen, Yu-Kun Lai, Hongbo Fu, Boxin Shi, and Lin Gao. 2024. Real-time 3d-aware portrait video relighting. In *Proceedings of the IEEE/CVF Conference on Computer Vision and Pattern Recognition*. 6221–6231.

Eric R Chan, Connor Z Lin, Matthew A Chan, Koki Nagano, Boxiao Pan, Shalini De Mello, Orazio Gallo, Leonidas J Guibas, Jonathan Tremblay, Sameh Khamis, et al. 2022. Efficient geometry-aware 3d generative adversarial networks. In *Proceedings of the IEEE/CVF conference on computer vision and pattern recognition*. 16123–16133.

Eric R Chan, Marco Monteiro, Petr Kellnhofer, Jiajun Wu, and Gordon Wetzstein. 2021. pi-gan: Periodic implicit generative adversarial networks for 3d-aware image synthesis. In *Proceedings of the IEEE/CVF conference on computer vision and pattern recognition*. 5799–5809.

Sumit Chaturvedi, Mengwei Ren, Yannick Hold-Geoffroy, Jingyuan Liu, Julie Dorsey, and Zhixin Shu. 2025. SynthLight: Portrait Relighting with Diffusion Model by Learning to Re-render Synthetic Faces. In *Proceedings of the Computer Vision and Pattern Recognition Conference*. 369–379.

Robert L Cook and Kenneth E Torrance. 1981. A reflectance model for computer graphics. *ACM Siggraph Computer Graphics* 15, 3 (1981), 307–316.

Paul Debevec, Tim Hawkins, Chris Tchou, Haarm-Pieter Duiker, Westley Sarokin, and Mark Sagar. 2000. Acquiring the reflectance field of a human face. In *Proceedings of the 27th annual conference on Computer graphics and interactive techniques*. 145–156.

Boyang Deng, Yifan Wang, and Gordon Wetzstein. 2024. Lumigan: Unconditional generation of relightable 3d human faces. In *2024 International Conference on 3D Vision (3DV)*. IEEE, 302–312.

Yu Deng, Jiaolong Yang, Dong Chen, Fang Wen, and Xin Tong. 2020. Disentangled and controllable face image generation via 3d imitative-contrastive learning. In *Proceedings of the IEEE/CVF conference on computer vision and pattern recognition*. 5154–5163.

Fan Fei, Yean Cheng, Yongjie Zhu, Qian Zheng, Si Li, Gang Pan, and Boxin Shi. 2024. SPLiT: Single Portrait Lighting Estimation via a Tetrad of Face Intrinsics. *IEEE Transactions on Pattern Analysis and Machine Intelligence* 46, 02 (feb 2024), 1079–1092. doi:10.1109/TPAMI.2023.3328453

Yao Feng, Haiwen Feng, Michael J Black, and Timo Bolkart. 2021. Learning an animatable detailed 3D face model from in-the-wild images. *ACM Transactions on Graphics (ToG)* 40, 4 (2021), 1–13.

Mingtao Guo, Guanyu Xing, and Yanli Liu. 2025a. High-Fidelity Relightable Monocular Portrait Animation with Lighting-Controllable Video Diffusion Model. In *Proceedings of the Computer Vision and Pattern Recognition Conference*. 228–238.

Mingtao Guo, Guanyu Xing, and Yanli Liu. 2025b. High-Fidelity Relightable Monocular Portrait Animation with Lighting-Controllable Video Diffusion Model. In *Proceedings of the Computer Vision and Pattern Recognition Conference (CVPR)*. 228–238.

Andrew Hou, Michel Sarkis, Ning Bi, Yiyang Tong, and Xiaoming Liu. 2022. Face relighting with geometrically consistent shadows. In *Proceedings of the IEEE/CVF conference on computer vision and pattern recognition*. 4217–4226.

Kaiwen Jiang, Shu-Yu Chen, Hongbo Fu, and Lin Gao. 2023. Nerffaelighting: Implicit and disentangled face lighting representation leveraging generative prior in neural radiance fields. *ACM Transactions on Graphics* 42, 3 (2023), 1–18.

Kaiwen Jiang, Feng-Lin Liu, Shu-Yu Chen, Pengfei Wan, Yuan Zhang, Yu-Kun Lai, Hongbo Fu, and Lin Gao. 2025. NerFFaceShop: learning a photo-realistic 3D-aware generative model of animatable and relightable heads from large-scale in-the-wild videos. *IEEE Transactions on Visualization and Computer Graphics* (2025).

Tero Karras, Samuli Laine, and Timo Aila. 2019. A style-based generator architecture for generative adversarial networks. In *Proceedings of the IEEE/CVF conference on computer vision and pattern recognition*. 4401–4410.

Vahid Kazemi and Josephine Sullivan. 2014. One millisecond face alignment with an ensemble of regression trees. In *Proceedings of the IEEE conference on computer vision and pattern recognition*. 1867–1874.

Bernhard Kerbl, Georgios Kopanas, Thomas Leimkühler, and George Drettakis. 2023. 3D Gaussian splatting for real-time radiance field rendering. *ACM Trans. Graph.* 42, 4 (2023), 139–1.

Hoon Kim, Minje Jang, Wonjun Yoon, Jisoo Lee, Donghyun Na, and Sanghyun Woo. 2024. Switchlight: Co-design of physics-driven architecture and pre-training framework for human portrait relighting. In *Proceedings of the IEEE/CVF Conference on Computer Vision and Pattern Recognition*. 25096–25106.

Alexander Kirillov, Eric Mintun, Nikhila Ravi, Hanzi Mao, Chloe Rolland, Laura Gustafson, Tete Xiao, Spencer Whitehead, Alexander C Berg, Wan-Yen Lo, et al. 2023. Segment anything. In *Proceedings of the IEEE/CVF international conference on computer vision*. 4015–4026.

Tobias Kirschstein, Simon Giebenhain, Jiapeng Tang, Markos Georgopoulos, and Matthias Nießner. 2024. Gghead: Fast and generalizable 3d gaussian heads. In *SIGGRAPH Asia 2024 Conference Papers*. 1–11.

Junxuan Li, Chen Cao, Gabriel Schwartz, Rawal Khirodkar, Christian Richardt, Tomas Simon, Yaser Sheikh, and Shunsuke Saito. 2024. Uravatar: Universal relightable gaussian codec avatars. In *SIGGRAPH Asia 2024 Conference Papers*. 1–11.

Henglei Lv, Bailin Deng, Jianzhu Guo, Xiaoliang Liu, Pengfei Wan, Di Zhang, and Lin Gao. 2025. GSHeadRelight: Fast relightability for 3D gaussian head synthesis. In *Proceedings of the Special Interest Group on Computer Graphics and Interactive Techniques Conference Conference Papers*. 1–12.

Yiqun Mei, Mingming He, Li Ma, Julien Philip, Wengqi Xian, David M George, Xueming Yu, Gabriel Dedic, Ahmet Levent Taşel, Ning Yu, Vishal M Patel, and Paul Debevec. 2025. Lux Post Facto: Learning Portrait Performance Relighting with Conditional Video Diffusion and a Hybrid Dataset. In *Proceedings of the IEEE/CVF Conference on Computer Vision and Pattern Recognition (CVPR)*. 5510–5522.

Yiqun Mei, Yu Zeng, He Zhang, Zhixin Shu, Xuaner Zhang, Sai Bi, Jianming Zhang, HyunJoon Jung, and Vishal M Patel. 2024. Holo-Relighting: Controllable Volumetric Portrait Relighting from a Single Image. In *Proceedings of the IEEE/CVF Conference on Computer Vision and Pattern Recognition*. 4263–4273.

Yiqun Mei, He Zhang, Xuaner Zhang, Jianming Zhang, Zhixin Shu, Yilin Wang, Zijun Wei, Shi Yan, HyunJoon Jung, and Vishal M Patel. 2023. Lightpainter: Interactive portrait relighting with freehand scribble. In *Proceedings of the IEEE/CVF conference on computer vision and pattern recognition*. 195–205.

Ben Mildenhall, Pratul P Srinivasan, Matthew Tancik, Jonathan T Barron, Ravi Ramamoorthi, and Ren Ng. 2021. Nerf: Representing scenes as neural radiance fields for view synthesis. *Commun. ACM* 65, 1 (2021), 99–106.

Xingang Pan, Xudong Xu, Chen Change Loy, Christian Theobalt, and Bo Dai. 2021. A shading-guided generative implicit model for shape-accurate 3d-aware image synthesis. *Advances in Neural Information Processing Systems* 34 (2021), 20002–20013.

Rohit Pandey, Sergio Orts-Escolano, Chloe Legendre, Christian Haene, Sofien Bouaziz, Christoph Rhemann, Paul E Debevec, and Sean Ryan Fanello. 2021. Total relighting: learning to relight portraits for background replacement. *ACM Trans. Graph.* 40, 4 (2021), 43–1.

Pascal Paysan, Reinhard Knothe, Brian Amberg, Sami Romdhani, and Thomas Vetter. 2009. A 3D face model for pose and illumination invariant face recognition. In *2009 sixth IEEE international conference on advanced video and signal based surveillance*. Ieee, 296–301.

Puntawat Ponglerntapakorn, Nontawat Tritrong, and Supasorn Suwajanakorn. 2023. Difareli: Diffusion face relighting. In *Proceedings of the IEEE/CVF international conference on computer vision*. 22646–22657.

Anurag Ranjan, Kwang Moo Yi, Jen-Hao Rick Chang, and Oncel Tuzel. 2023. Facelit: Neural 3d relightable faces. In *Proceedings of the IEEE/CVF Conference on Computer Vision and Pattern Recognition*. 8619–8628.

Pramod Rao, Gereon Fox, Abhimitra Meka, Mallikarjun BR, Fangneng Zhan, Tim Weyrich, Bernd Bickel, Hanspeter Pfister, Wojciech Matusik, Mohamed Elgharib, et al. 2024. Lite2Relight: 3D-aware Single Image Portrait Relighting. In *ACM*

SIGGRAPH 2024 Conference Papers. 1–12.

Pramod Rao, Abhimitra Meka, Xilong Zhou, Gereon Fox, Fangneng Zhan, Tim Weyrich, Bernd Bickel, Hanspeter Pfister, Wojciech Matusik, Thabo Beeler, et al. 2025. 3DPR: Single Image 3D Portrait Relight using Generative Priors. *arXiv preprint arXiv:2510.15846* (2025).

Daniel Roich, Ron Mokady, Amit H Bermano, and Daniel Cohen-Or. 2022. Pivotal tuning for latent-based editing of real images. *ACM Transactions on graphics (TOG)* 42, 1 (2022), 1–13.

Shunsuke Saito, Gabriel Schwartz, Tomas Simon, Junxuan Li, and Giljoo Nam. 2024. Relightable gaussian codec avatars. In *Proceedings of the IEEE/CVF Conference on Computer Vision and Pattern Recognition*. 130–141.

Christophe Schlick. 1994. An inexpensive BRDF model for physically-based rendering. In *Computer graphics forum*. Vol. 13. 233–246.

Katja Schwarz, Yiyi Liao, Michael Niemeyer, and Andreas Geiger. 2020. Graf: Generative radiance fields for 3d-aware image synthesis. *Advances in neural information processing systems* 33 (2020), 20154–20166.

Alon Shoshan, Nadav Bhowmik, Igor Kvirkavsky, and Gerard Medioni. 2021. Gan-control: Explicitly controllable gans. In *Proceedings of the IEEE/CVF international conference on computer vision*. 14083–14093.

Peter-Pike J Sloan, Jan Kautz, and John M Snyder. 2002. Precomputed radiance transfer for real-time rendering in dynamic, low-frequency lighting environments. *ACM Trans. Graph.* (2002).

Jingxiang Sun, Xuan Wang, Lizhen Wang, Xiaoyu Li, Yong Zhang, Hongwen Zhang, and Yebin Liu. 2023. Next3d: Generative neural texture rasterization for 3d-aware head avatars. In *Proceedings of the IEEE/CVF conference on computer vision and pattern recognition*. 20991–21002.

Feitong Tan, Sean Fanello, Abhimitra Meka, Sergio Orts-Escolano, Danhang Tang, Rohit Pandey, Jonathan Taylor, Ping Tan, and Yinda Zhang. 2022. Volux-gan: A generative model for 3d face synthesis with hdri relighting. In *ACM SIGGRAPH 2022 Conference Proceedings*. 1–9.

Junshu Tang, Bo Zhang, Binxin Yang, Ting Zhang, Dong Chen, Lizhuang Ma, and Fang Wen. 2023. 3dfaceshop: Explicitly controllable 3d-aware portrait generation. *IEEE transactions on visualization and computer graphics* 30, 9 (2023), 6020–6037.

Timo Teufel, Pulkit Gera, Xilong Zhou, Umar Iqbal, Pramod Rao, Jan Kautz, Vladislav Golyanik, and Christian Theobalt. 2025. HumanOLAT: A Large-Scale Dataset for Full-Body Human Relighting and Novel-View Synthesis. In *Proceedings of the IEEE/CVF International Conference on Computer Vision (ICCV)*. 29131–29141.

TS Trowbridge and K P Reitz. 1975. Average irregularity representation of a rough surface for ray reflection. *J. Opt. Soc. Am.* 65, 5 (1975), 531–536.

Bruce Walter, Stephen R Marschner, Hongsong Li, and Kenneth E Torrance. 2007. Microfacet Models for Refraction through Rough Surfaces. *Rendering techniques* 2007 (2007), 18th.

Junying Wang, Jingyuan Liu, Xin Sun, Krishna Kumar Singh, Zhixin Shu, He Zhang, Jimei Yang, Nanxuan Zhao, Tuanfeng Y. Wang, Simon S. Chen, Ulrich Neumann, and Jae Shin Yoon. 2025. Comprehensive Relighting: Generalizable and Consistent Monocular Human Relighting and Harmonization. In *Proceedings of the IEEE/CVF Conference on Computer Vision and Pattern Recognition (CVPR)*. 380–390.

Yiming Wang, Qin Han, Marc Habermann, Kostas Daniilidis, Christian Theobalt, and Lingjie Liu. 2023. Neus2: Fast learning of neural implicit surfaces for multi-view reconstruction. In *Proceedings of the IEEE/CVF International Conference on Computer Vision*. 3295–3306.

Zhibo Wang, Xin Yu, Ming Lu, Quan Wang, Chen Qian, and Feng Xu. 2020. Single image portrait relighting via explicit multiple reflectance channel modeling. *ACM Transactions on Graphics (ToG)* 39, 6 (2020), 1–13.

Xiaoyan Xing, Konrad Groh, Sezer Karaoglu, Theo Gevers, and Anand Bhattad. 2025. LumiNet: Latent Intrinsic Meets Diffusion Models for Indoor Scene Relighting. In *Proceedings of the IEEE/CVF Conference on Computer Vision and Pattern Recognition (CVPR)*. 442–452.

Valikhujaev Yakhyaev. 2024. face-parsing. <https://github.com/yakhya/face-parsing>. GitHub repository.

Yu-Ying Yeh, Koki Nagano, Sameh Khamis, Jan Kautz, Ming-Yu Liu, and Ting-Chun Wang. 2022. Learning to relight portrait images via a virtual light stage and synthetic-to-real adaptation. *ACM Transactions on Graphics (TOG)* 41, 6 (2022), 1–21.

Ran Yi, Teng Hu, Mengfei Xia, Yizhe Tang, and Yong-Jin Liu. 2024. Feditnet++: Few-shot editing of latent semantics in gan spaces with correlated attribute disentanglement. *IEEE Transactions on Pattern Analysis and Machine Intelligence* (2024).

Zhengming Yu, Tianye Li, Jingxiang Sun, Omer Shapira, Seonwook Park, Michael Stengel, Matthew Chan, Xin Li, Wenping Wang, Koki Nagano, and Shalini De Mello. 2025. GAIA: Generative Animatable Interactive Avatars with Expression-conditioned Gaussians. In *ACM SIGGRAPH*.

Lvmin Zhang, Anyi Rao, and Maneesh Agrawala. 2025. Scaling in-the-wild training for diffusion-based illumination harmonization and editing by imposing consistent light transport. In *The Thirteenth International Conference on Learning Representations*.

Peng Zheng, Dehong Gao, Deng-Ping Fan, Li Liu, Jorma Laaksonen, Wanli Ouyang, and Nicu Sebe. 2024. Bilateral reference for high-resolution dichotomous image segmentation. *arXiv preprint arXiv:2401.03407* (2024).

Hao Zhou, Sunil Hadap, Kalyan Sunkavalli, and David W Jacobs. 2019. Deep single-image portrait relighting. In *Proceedings of the IEEE/CVF international conference on computer vision*. 7194–7202.



Figure 4: Relighting under complex environment maps. NFL assumes white illumination and fails to handle colored lighting. GSHR lacks real-world OLAT supervision and therefore cannot produce physically plausible responses under complex lighting. In contrast, our method, trained with multi-view OLAT captures, accurately renders realistic shading and reflections under diverse and challenging illumination conditions.

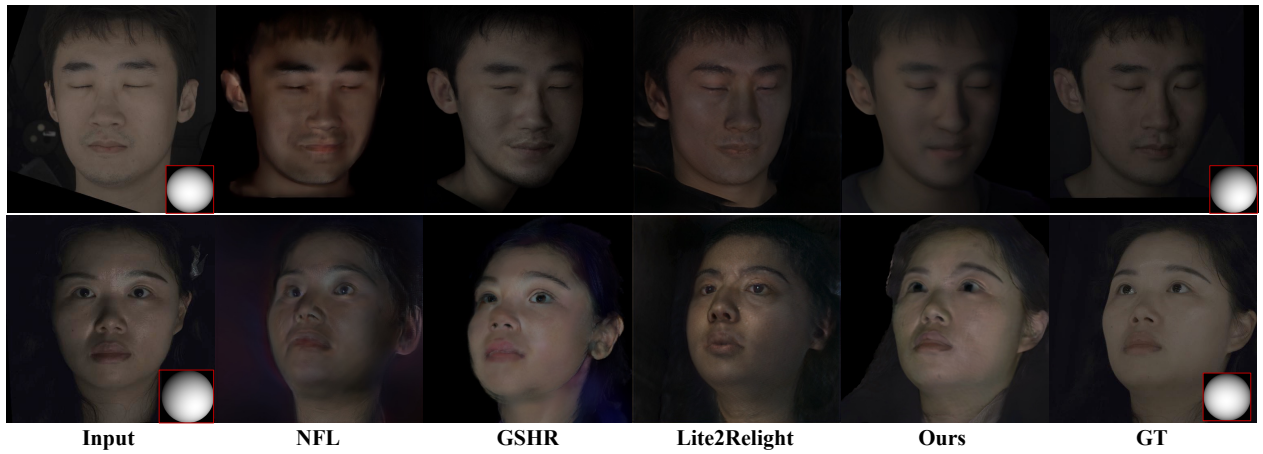


Figure 5: Free-view relighting on captured LightStage data. Compared with NFL, GSHR, and Lite2Relight, our method better disentangles lighting from intrinsic facial attributes by learning reflectance priors from OLAT data, leading to more realistic relighting from a single portrait image. We show the lighting condition of the image in the red boxes.



Figure 6: Effect of optimizing different layers for illumination removal. From left to right: original GGHead output, optimization of layer 6 only, layers 5+6, and full-model optimization. Optimizing only layer 6 fails to remove all lighting artifacts (e.g., sunglasses in row 1, left mouth corner in row 4). Full-model optimization significantly alters facial geometry (e.g., rows 2–3).

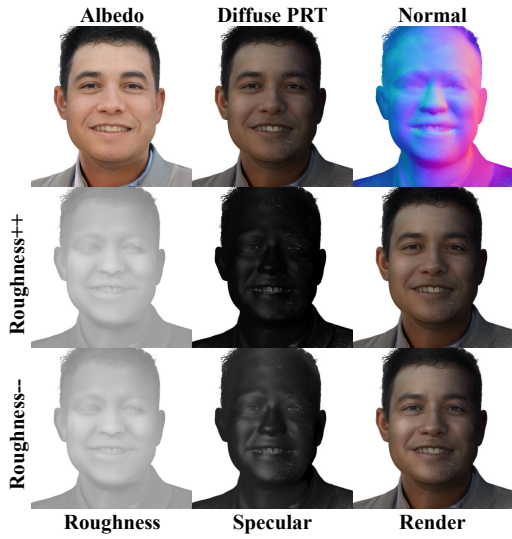


Figure 7: Explicit roughness editing. We demonstrate the editing of material roughness for the generated characters. By decreasing the roughness value (i.e., increasing smoothness), we achieve more pronounced specular highlights, as shown in the third row. Notably, the underlying geometry and albedo remain unchanged, highlighting the disentangled nature of our representation.

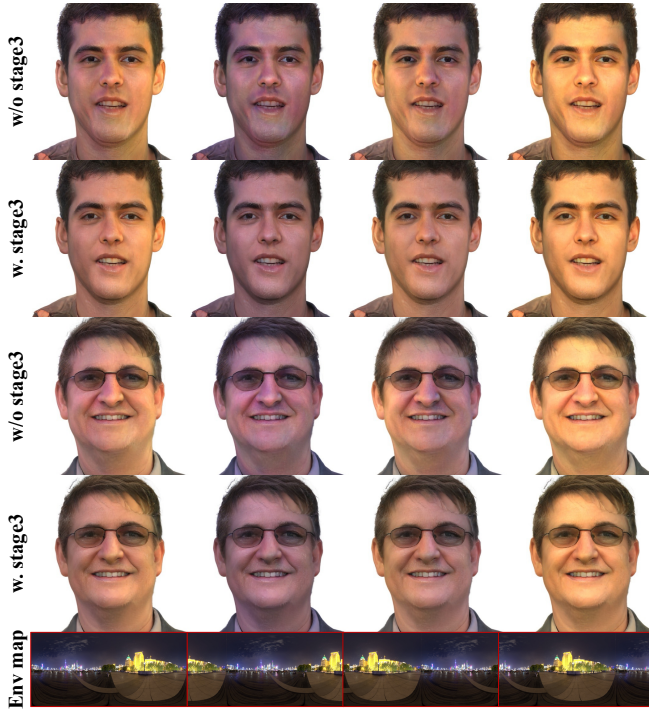


Figure 8: Ablation study on Stage 3. We rotate the environment map and render two randomly sampled 3D heads to evaluate the impact of Stage 3 adversarial training. Rows 1 and 3 show results without Stage 3 training. Under blue lighting—an illumination condition significantly different from the OLAT training distribution—models without Stage 3 exhibit noticeable artifacts. In contrast, Stage 3 training yields more plausible and robust relighting results.



Figure 9: Normal generation using different methods. From left to right: normals from averaged orientations of neighboring Gaussians, normals computed after mesh extraction, and our method. The first two approaches exhibit noticeable noise (highlighted in red boxes), while our method produces plausible and smooth normals.

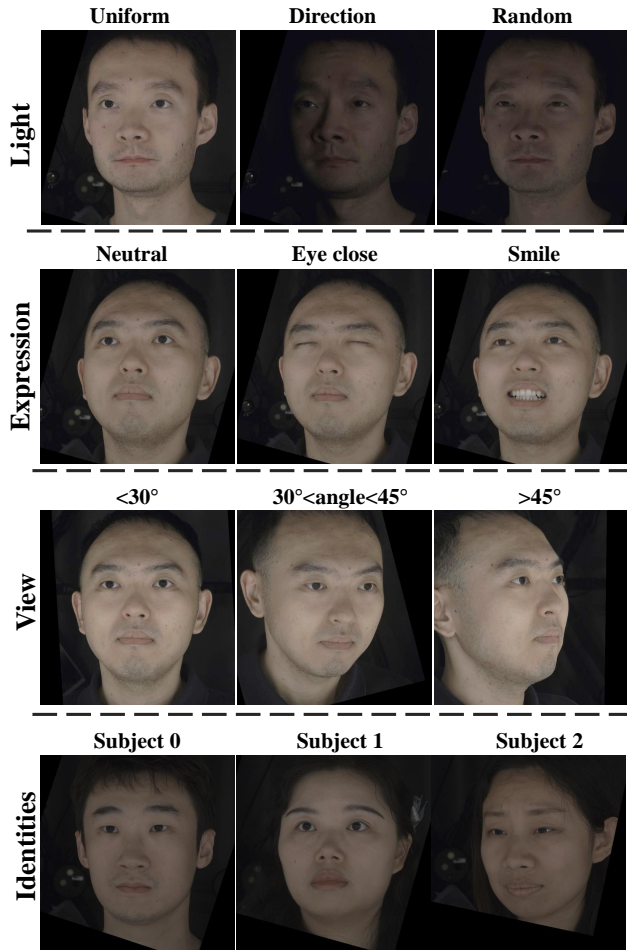


Figure 10: An overview of the lightstage captures.

6 Implementation Details

Dataset. We provide a summarized overview of the LightStage dataset in Fig 10. The dataset encompasses diverse subjects, lighting conditions, facial expressions, and viewing angles. The lighting conditions are categorized into three types: uniform, directional, and random. The facial expressions include neutral, smiling, and closed eyes.

Training. We provide hyper parameters and configurations of training in this section.

- **Stage1:** We retain the majority of the pretrained GGHead model’s architecture and parameters, and modify only the final layer to output RGB values instead of the original spherical harmonic coefficients. We fine-tune this modified model for 200k iterations on the FFHQ dataset using an adversarial loss. We then generate 10,000 pseudo-albedo images using NFL [Jiang et al. 2023]. To prevent identity collapse, we use a large truncated ψ value, which controls the diversity of sampled latent codes by constraining the sampling region in the latent space. We fine-tune the model for an additional 10,000 iterations on these pseudo-albedo images with an adversarial loss, removing the lighting component from the

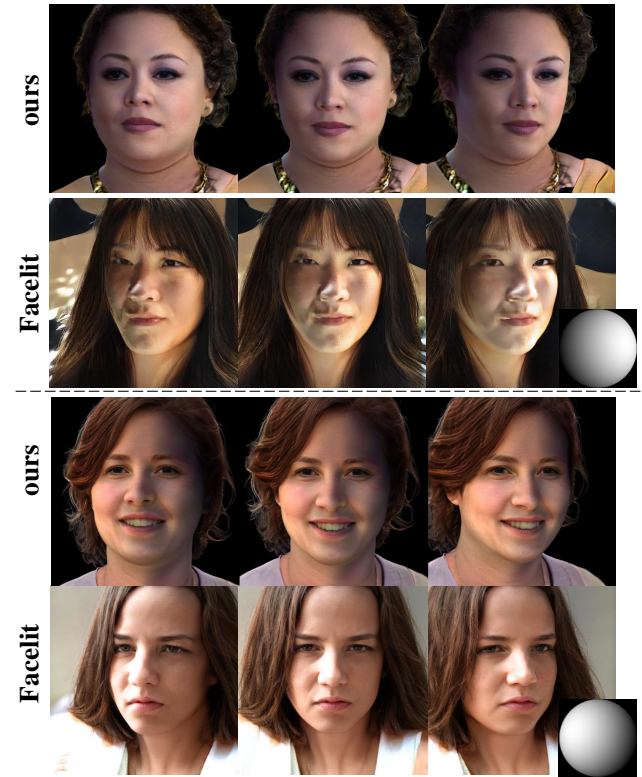


Figure 11: Comparisons with FaceLit [Ranjan et al. 2023].

pretrained GGHead model while maintaining the diversity of the generated identities.

- **Stage2-Inversion:** We achieve multi-view inversion under the supervision of multiple loss terms. We set the weight of the \mathcal{L}_2 to 0.1, the weight of the \mathcal{L}_{perc} to 1, and the weight of \mathcal{L}_{tv} to 0.01. We compute the perceptual loss only using frontal images. The inversion process requires 500 iterations, and the inversion result of the previous fully lit frame serves as the initial value for the next frame to accelerate convergence.
- **Network:** We employ a lightweight network including 2 layers and Leaky ReLU activation to enable multi-scale features of G_{base} to guide the relight branch. We design G_{relit} with a reduced feature dimensionality: its convolutional layers operate on 256-dimensional features, compared to 512 in G_{base} . Finally, the relight branch requires approximately 90 MB memory storage.
- **Stage2-Training:** We set weights of \mathcal{L}_{normal}^D , $\mathcal{L}_{normal}^{TV}$ to be 1 and 10 respectively. The weights of \mathcal{L}_{img} , \mathcal{L}_{perc} and \mathcal{L}_{tv}^I are 0.1, 1, 1. And weight of \mathcal{L}_{prt} is set to 10.
- **Stage3-Training:** Firstly, we train mapping network M_{lit} for 10k iterations. Then we train the relight branch using adversarial loss with a small learning rate $1e - 6$. The parameters of discriminator are fixed.

Finetune	Identity Similarity
Layer 6	0.9685
Layer 5+6	0.9654
All Layers	0.9599

Table 4: Quantitative comparison of identity preservation when fine-tuning different StyleGAN layers, measured by average cosine similarity (higher is better) between generated faces and the original GGHead output using the face_recognition library.

7 More Experiments

Comparison with FaceLit We also provide comparisons with FaceLit [Ranjan et al. 2023] in Fig 11. FaceLit is unsupervised disentanglement method based on volume rendering, which struggle with extreme lighting conditions and often produce unrealistic lighting artifacts. Moreover, it relies on a white-light assumption and therefore cannot handle colored lighting. In contrast, our method supports diverse lighting inputs, including color environment maps, point lights, and spherical harmonic coefficients. It also produces natural lighting and shadow effects even under strong side lighting conditions.

Ablation Study on Base Branch Adaption. We quantitatively evaluated identity preservation when fine-tuning different layers of StyleGAN. Specifically, we randomly generated 100 images and used the face_recognition library to compute the facial embedding for each image. We then measured the similarity between images produced by GGHead and those generated by three variants using the same latent codes: (1) fine-tuning only layer 6; (2) fine-tuning layers 5 and 6; and (3) fine-tuning all layers. As shown in the table 4, the results indicate that fine-tuning the entire model significantly alters facial identity, whereas fine-tuning only layer 6 or layers 5+6 preserves identity to a similar degree. However, qualitative results show that optimizing only layer 6 still introduces noticeable lighting artifacts. Therefore, we chose to optimize layers 5 and 6 jointly.

8 Limitations.

The model is static and does not support the control of facial expressions. Furthermore, the number of captured identities and lighting conditions remains limited, which restricts the model’s ability to learn a more comprehensive prior over diverse facial material properties. Future work could address these by incorporating video captures and expanding the dataset scale.

9 Ethical Considerations

The generation of artificial portrait using our method poses risks, including the spread of false information, and erosion of trust in media credibility. These issues could have profound societal implications. Addressing this challenge requires developing reliable techniques to identify and verify authentic content.